Paclitaxel and Nocodazole Differentially Alter Endocytosis in Cultured Cells

Sarah F. Hamm-Alvarez,[1,2] Manisha Sonee,[1] Kathleen Loran-Goss,[1] and Wei-Chiang Shen[1]

Received May 29, 1996; accepted August 12, 1996

Purpose. Microtubule-based transport facilitates the endocytosis of exogenous macromolecules. We have determined how microtubule accumulation and disassembly alter endocytosis.

Methods. The effects of paclitaxel, which promotes microtubule assembly, and nocodazole, which promotes microtubule disassembly, on fluid-phase and receptor-mediated endocytosis were measured using uptake of horseradish peroxidase and ^{125}I-transferrin, respectively. Changes in membrane and microtubule organization were examined by fluorescence microscopy.

Results. Neither paclitaxel (4 μM, 60 min pretreatment) nor nocodazole (1 μg/ml, 60 min pretreatment) significantly inhibited fluid-phase endocytosis. However, paclitaxel caused a redistribution of fluorescent fluid-phase marker to the periphery. Both paclitaxel and nocodazole treatment significantly ($p \leq 0.05$) reduced the initial uptake of ^{125}I-transferrin at 5 min to ~50% of control. Despite the similarity of the effects on initial endocytic uptake, the effects on steady state accumulation of ^{125}I-transferrin were quite distinct. Exposure of CV-1 cells to paclitaxel for an additional 30, 60 or 90 min also showed reduced accumulation of ^{125}I-transferrin up to a maximum significant ($p \leq 0.05$) inhibition of 48% ± 10% of control at 90 min. In contrast, nocodazole caused an initial significant ($p \leq 0.05$) increase in ^{125}I-transferrin accumulation after 30 min (159% ± 13% of control), while by 90 min ^{125}I-transferrin accumulation had returned to control levels. Microtubule content, particularly of stable microtubules, was increased in CV-1 cells by paclitaxel, but abolished by nocodazole treatment.

Conclusions. Our data show that changes in the microtubule array can alter the dynamics of receptor movement through the endosomal pathway. However, microtubule assembly versus disassembly have different effects.

KEY WORDS: microtubule; paclitaxel; nocodazole; endocytosis; drug delivery.

INTRODUCTION

The cellular microtubule (MT) network supports the movement of cellular membrane vesicles driven primarily by two cytoplasmic motor proteins, kinesin and cytoplasmic dynein (reviewed in 1). An increasing body of evidence suggests that these membrane vesicle movements facilitate membrane traffic involved in endocytosis and secretion (reviewed in 2). Paclitaxel is known to promote MT assembly (3), even in the absence of factors usually essential for polymerization (GTP, MT-associated proteins) and in the presence of conditions that normally promote disassembly (Ca^{2+}, cold). Treatment of cells with paclitaxel results in inhibition of MT-dependent vesicle movements (4); however, the identity of these vesicles and their role in membrane traffic has not been previously defined. Nocodazole, which results in loss of cellular MTs (5) has also been utilized to examine the role for MT-dependent transport in membrane trafficking. We have previously observed that several parameters of small vesicle movement in CV-1 cells that were sensitive to paclitaxel were also inhibited by nocodazole treatment (4), suggesting that paclitaxel and nocodazole might impact similarly on membrane traffic.

To explore the effects of changes in cellular MT content on membrane traffic involved in endocytosis and recycling, we have measured the effects of paclitaxel and nocodazole on fluid-phase endocytosis, using horseradish peroxidase (HRP) as a marker. We have also measured the effects of paclitaxel on receptor-mediated endocytosis using the transferrin (Tf)-transferrin receptor (TfR) model. TfR binds Tf at the plasma membrane, triggering internalization via receptor-mediated endocytosis (reviewed in 6). Once internalized, the complex is transported to endosomes where release of Fe^{3+} from Tf is facilitated by the decreased pH of the endosomal system. Most apoTf-TfR complex is recycled directly from endosomal compartments to the plasma membrane where apoTf is released. Studies also support a longer Tf-TfR recycling pathway through the Golgi complex (7–9) which appears to involve MT-based transport (10–12).

We were particularly interested in using the Tf-TfR model to examine whether MT assembly versus MT disassembly had different effects on receptor movement because it has been considered as a vehicle for delivery of polar drugs including antisense and gene therapy into cells (13–14). MTs within many cells exist as subpopulations, some of which exchange more rapidly with free tubulin and others which are more static. Several posttranslational modifications on α-tubulin, e.g. detyrosination and acetylation, have been reported which distinguish more stable MTs from dynamic MTs (reviewed in 15). Effects of the MT-targeted drugs on HRP uptake and Tf accumulation were correlated with changes observed in membrane organization and MT subpopulation distribution. Our results demonstrate that MT assembly versus MT disassembly have distinct effects on endocytosis of TfR.

MATERIALS AND METHODS

Reagents

Paclitaxel was obtained from LC Laboratories (Woburn, MA). Monensin was obtained from Calbiochem. Nocodazole, HRP, human apotransferrin, mouse monoclonal anti-acetylated α-tubulin antibody (clone 6-11B-1), FITC-labeled goat anti-mouse and goat-anti rat secondary antibodies and FITC-BSA were obtained from Sigma Chemical Co. Rhodamine-labeled wheat germ agglutinin (WGA) was obtained from Molecular Probes. The monoclonal antibody, ID4B, developed by Dr. Thomas August was obtained from the Developmental Studies Hybridoma Bank, maintained by the Department of Pharmacology and Molecular Sciences, Johns Hopkins University School of Medicine, Baltimore, MD 21205, and the Department of Biological Sciences, University of Iowa, Iowa City, IA 52242,

[1] Department of Pharmaceutical Sciences, USC School of Pharmacy, Los Angeles, California 90033.

[2] To whom correspondence should be addressed.

ABBREVIATIONS: MT, microtubule; Tf, transferrin; TfR, transferrin receptor; HRP, horseradish peroxidase; LAMP, lysosomal acidic membrane protein; MTOC, microtubule organizing center.

0724-8741/96/1100-1647$09.50/0 © 1996 Plenum Publishing Corporation

under contract N01-HD-2-3144 from the NICHD. The rat monoclonal anti-α tubulin antibody (YOL1/34) was purchased from Accurate Scientific (Westbury, NY). All cell culture reagents were obtained from Gibco-BRL.

Cell Culture

CV-1 (African green monkey kidney) cells were obtained from ATCC and maintained in Minimal Essential Medium (Earle's salts) containing 10% FBS, and penicillin/streptomycin at 37°C in a 5% CO_2 incubator. 3T3 cells were also obtained from ATCC and maintained in Dulbecco's Modified Eagle Medium (low glucose) containing 10% FBS and penicillin/streptomycin at 37°C in a 5% CO_2 incubator. Both cell types were split at confluence using trypsin/EDTA.

Cell Treatments

For all assays, cells grown on coverslips or in 6-well plates were exposed to the drug for the indicated times at 37°C in a 5% CO_2 incubator in conditioned media. Pretreatments with paclitaxel (4 μM), monensin (4.6 μM) and nocodazole (1 μg/ml) were for 60 min. Prior to nocodazole treatment, cells were cooled for 5 min on ice (4). The doses of paclitaxel and nocodazole were chosen based on a previous study which demonstrated that the expected changes in the MT array were correlated with inhibition of MT-based vesicle transport following exposure of CV-1 cells to these doses and times (4). The same concentrations of each drug were maintained throughout the duration of the uptake assays for HRP and Tf.

Immunofluorescence Microscopy

For immunofluorescence microscopy, cells were seeded onto sterile glass coverslips. All slides were observed and photographed using a Zeiss Axioskop equipped with a 63× objective attached to an MC-100 spot camera. Fixation and staining of MTs was according to methods described previously (4). Fixation and staining of lysosomal membranes with the monoclonal antibody, ID4B, to the lysosomal acidic membrane protein 1 (LAMP-1) in 3T3 cells was based on methods previously described (16).

For uptake experiments with FITC-BSA, control and treated CV-1 cells were exposed to FITC-BSA (1 mg/ml) in medium and incubated for the indicated times at 37°C at 5% CO_2. The cells were cooled on ice for 5 min, rinsed 3× in ice cold DPBS, and fixed in 4% paraformaldehyde (Sigma) in DPBS for 15 min. Cells were then rinsed in DPBS, exposed to 50 mM NH_4Cl in DPBS for 5 min, rinsed in DPBS, and mounted in Vectashield mounting medium (Vector Laboratories Inc, Burlingame CN).

Fluid-Phase Uptake Measurements

CV-1 cells were seeded into 6 well plates such that they reached confluence within 48–72 hrs. For uptake measurements, cells were pretreated as described above prior to addition of HRP at 300 μg/ml in fresh complete medium with and without the treatments of interest. Cells were incubated with HRP-containing media for 90 min at 37°C at 5% CO_2. The plates were then placed on ice for 5 min to block fluid phase uptake and recycling prior to washing in ice cold PBS 3×. Cells were then dissolved in 1.0 ml of 0.1% Triton X-100 in distilled water and HRP activity was determined as described (17). Cell samples (0.5 ml) were diluted into 1.0 ml of developing solution (containing 100 μg/ml of *o*-dianisidine and 0.02% H_2O_2) and the rate of product formation was measured at 460 nm in a spectrophotometer. An aliquot of the dissolved cells was also removed for protein assay in 96-well plates using the Micro-BCA kit (Pierce). Values for HRP activity (units/min) in cells from each well were normalized to protein.

Preparation of ^{125}I-Tf

ApoTf was loaded with iron by the method of Larrick and Cresswell (18). The Tf was then labeled using $Na^{125}I$ (ICN, 100 mCi/ml, carrier free) with iodobeads (Pierce) according to the manufacturer's instructions and as previously described (19). Labeled ^{125}I-Tf at a concentration of 0.2 mCi/mg transferrin was stored at −20°C and used within 6 weeks.

^{125}I-Tf Uptake/Recycling Experiments

CV-1 or 3T3 cells were seeded into 6 well plates such that they reached confluence and were assayed within 48–72 hrs. Prior to assays, the complete medium was replaced with Minimal Essential Medium, Earle's salts, containing 1% BSA (Sigma, Fraction V) and penicillin/streptomycin for 12–18 hours in order to enrich membrane concentrations of TfR. Cells were pretreated as described above and prior to addition of fresh media containing ^{125}I-Tf (1μg/ml). For competitive binding determinations, unlabeled Tf at an approximately 350-fold molar excess (0.35 mg/ml) was added. For uptake assays, incubations were at the indicated times at 37°C in a 5% CO_2 incubator. The plates were then cooled on ice for 5 min, rinsed 3× in ice-cold DPBS, and dissolved by addition of 1 ml of 0.1% Triton X-100 in distilled water to each well prior to incubation at 37°C. For measurement of plasma membrane TfR content following pretreatment with paclitaxel (4 μM) or nocodazole (1 μg/ml), cells were cooled to 4°C and ^{125}I-Tf with and without excess unlabeled Tf was added for 90 min. Plates were then processed as described above. Total radioactivity was measured in a Hewlett Packard gamma counter and normalized to protein (assayed by the Pierce Micro-BCA kit). The difference between the binding of ^{125}I-Tf and ^{125}I-Tf plus a large excess of unlabeled Tf to the cells was considered to be the TfR-specific binding of ^{125}I-Tf.

Statistics

For Tf uptake and binding assays, raw data values were compared by paired t-test with data considered significant at $p \leq 0.05$. For HRP uptake assays, normalized data values were compared by t-test with differences considered significant at $p \leq 0.05$.

RESULTS

Fluid-Phase Endocytosis Is Not Significantly Altered by MT-targeted Drugs

We first compared the effects of paclitaxel and nocodazole on endocytosis by measuring the uptake of HRP, a fluid-phase marker, under steady state conditions in confluent control and

Table I. CV-1 Cell Uptake of Horseradish Peroxidase

Treatments	37°C (% of control)	4°C (% of control)
Paclitaxel	114 ± 7%	107 ± 8%
Nocodazole	96 ± 7%	99 ± 7%
Monensin	71 ± 5%	114 ± 18%

Note: Paclitaxel treatment was at 4 μM, nocodazole at 1 μg/ml, and monensin was 4.6 μM. Results represent 3–8 experiments per point, expressed as mean ± s.e.m. Each experiment consists of a composite of 3–6 values per/treatment. Control cells were exposed to vehicle controls under the same conditions as the treatment.

treated CV-1 cells. The ionophore, monensin has been reported to inhibit the endocytotic uptake of HRP (20) in a MT-independent manner; we used monensin as a probe to confirm that the parameters of fluid-phase uptake in CV-1 cells were comparable to other systems.

Table I shows the effects of these treatments on HRP uptake. Values are shown under conditions which facilitated uptake (37°C) and non-specific association (4°C). Although paclitaxel increased HRP uptake slightly, this difference was not significant and may be attributable to the slight increase in non-specific binding in paclitaxel-treated cells (4°C). Nocodazole-treated CV-1 cells also showed no significant increases in either uptake (37°C) or non-specific binding (4°C), consistent with previous studies reporting little effect on fluid-phase endocytosis by colchicine and related compounds (reviewed in 21). As expected, monensin reduced HRP uptake to 71% ± 5%, consistent with previous reports (20, 22).

Paclitaxel But Not Nocodazole Reduces Accumulation of ^{125}I-Tf at Steady State

We first established the steady state parameters of Tf uptake in control CV-1 cells. Figure 1 shows the time course for ^{125}I-Tf uptake and accumulation in CV-1 cells. It is clear that following 30 min of exposure to ^{125}I-Tf, that the accumulation was close to steady state levels; these levels were maintained up to 90 min.

We therefore chose to first assess accumulation of ^{125}I-Tf at 90 min, since ^{125}I-Tf accumulation was clearly at steady state at this time point, as indicated in Figure 1. In addition to its inhibition of fluid-phase uptake, monensin has previously been shown to inhibit traffic and movement of receptors including TfR from the Golgi compartment (22, 23). In order to obtain additional information about TfR recycling in CV-1 cells relative to other cells, we measured the impact of monensin on TfR accumulation. Consistent with previous studies, we found that ^{125}I-Tf accumulation following 90 min of exposure was increased, consistent with a block in internalized ^{125}I-Tf movement through Golgi compartments (Figure 2). These data support the existence of a longer TfR recycling pathway through a Golgi or trans-Golgi network compartment in CV-1 cells.

When we examined the impact of the MT-targeted drugs on ^{125}I-Tf accumulation at 90 min in order, we found that paclitaxel significantly ($p \leq 0.05$) inhibited the cellular accumulation of ^{125}I-Tf following 90 min of exposure (Figure 2). Nocodazole, which promotes MT disassembly, had a different effect; as shown in Figure 2, no significant changes in accumulation of ^{125}I-Tf were seen following 90 min of exposure (Figure 2). Control experiments showed that nocodazole and paclitaxel did not cause major changes in the binding affinity of TfR for ^{125}I-Tf: binding of ^{125}I-Tf in the presence of paclitaxel was 114% ± 8% (n = 3) and in the presence of nocodazole was 92% ± 7% (n = 4). These data demonstrate that the changes in accumulation patterns of ^{125}I-Tf in nocodazole versus paclitaxel-treated cells are due to changes in the movement of TfR within the treated cells.

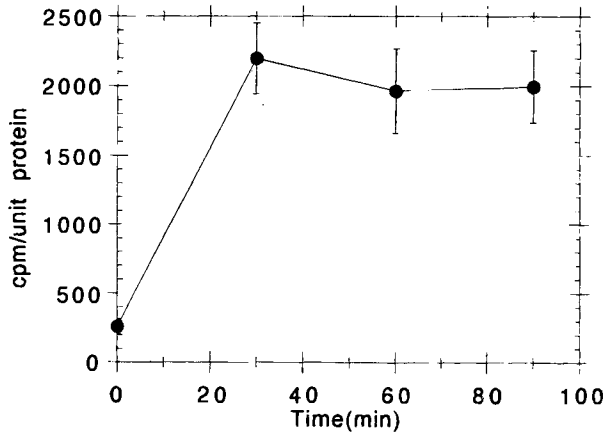

Fig. 1. Uptake of ^{125}I-Tf with increasing length of incubation reaches a steady state. ^{125}I-Tf (with and without unlabeled Tf) at concentrations indicated in Methods was added to CV-1 cell monolayers and incubated for the indicated times. Cells were rinsed extensively in ice-cold DPBS and dissolved prior to determination of protein content and associated cpm as described in Methods. Results represent mean ± s.e.m. of n = 3 separate experiments.

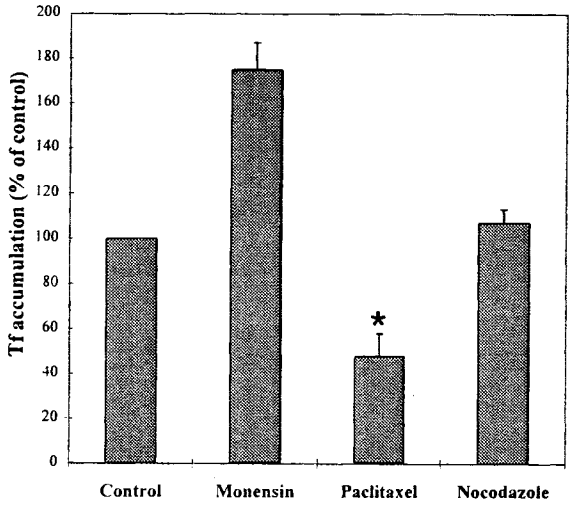

Fig. 2. Effect of paclitaxel, nocodazole and monensin on ^{125}I-Tf accumulation after 90 min of uptake. Accumulation of ^{125}I-Tf (specific binding) was determined in control and treated (60 min pretreatment, paclitaxel at 4 μM, nocodazole at 1 μg/ml and monensin at 4.6 μM) cells following 90 min exposure to ^{125}I-Tf in the presence and absence of unlabeled Tf. Radioactivity was normalized to protein yields and then normalized to control values. Results are expressed as ^{125}I-Tf accumulation (% of control) ± s.e.m., n = 4–10 assays per treatment. *Indicates values significant at $p \leq 0.05$.

MT-targeted Drugs Alter the Amount of TfR in the Plasma Membrane During Pretreatment

One contribution to the reduction in ^{125}I-Tf accumulation in paclitaxel-treated monolayers might be a reduction of plasma membrane content of TfR during paclitaxel pretreatment. We have measured the amount of TfR in the plasma membrane following paclitaxel and nocodazole pretreatment for 60 min, followed by cooling and measurement of binding at 4°C. At 4°C, all membrane traffic to and from the plasma membrane is blocked and ^{125}I-Tf binding can only occur with TfR already exposed to the cell exterior (plasma membrane TfR). We found that the level of TfR in the plasma membrane following paclitaxel pretreatment was reduced (Table II). Although nocodazole showed no effect on steady state accumulation of ^{125}I-Tf at 90 min, we also measured the composition of TfR in the plasma membrane following nocodazole pretreatment; nocodazole actually caused a slight but not significant increase in the amount of TfR in the plasma membrane (Table II).

Paclitaxel-induced Inhibition of Accumulation of ^{125}I-Tf Increases Over Time

Additionally, we examined whether the time course of accumulation of ^{125}I-Tf was altered prior to 90 min of exposure to ^{125}I-Tf with either paclitaxel or nocodazole; these results are shown in Figure 3. We first measured the ^{125}I-Tf accumulation after 5 min of uptake; this measurement reflects only Tf-TfR uptake and not recycling, unlike our other steady state measurements. As shown in Figure 3, both paclitaxel and nocodazole pretreatment significantly ($p \leq 0.05$) reduced the accumulation of ^{125}I-Tf at this early time point.

We also examined the steady state accumulation of ^{125}I-Tf at earlier steady state time points relative to 90 min. In paclitaxel-treated cells, only a small difference in the accumulation of ^{125}I-Tf in paclitaxel-treated cells relative to controls was detectable at 30 min (Figure 3). The inhibitory effect of paclitaxel on ^{125}I-Tf accumulation was more pronounced at 60 min (Figure 3) relative to the 30 min uptake values. As shown in Figure 2, by 90 min of exposure to ^{125}I-Tf, accumulation had fallen to <50% of controls in paclitaxel-treated cells.

We were surprised by the results with our comparable investigation with nocodazole, since no significant differences in accumulation were measured after 90 min uptake (Figure 2). In contrast to paclitaxel, in nocodazole-treated cells the accumulation of ^{125}I-Tf at 30 min was increased significantly relative to controls (Figure 3). An increase was also seen after 60 min of uptake in the presence of nocodazole, although it was not significant (Figure 3). However, values had returned to control levels by 90 min of exposure. This finding suggests that the intracellular accumulation of ^{125}I-Tf is actually enhanced by nocodazole for a short period, despite the reduced amount of initial accumulation seen after 5 min.

Table II. The Amount of TfR in the Plasma Membrane Following Paclitaxel and Nocodazole Is Altered

Pretreatment	Amount of TfR in the plasma membrane (% of control)
Paclitaxel	82 ± 4% (n = 4)
Nocodazole	120 ± 15% (n = 3)

Note: Pretreatment refers to a 60 min exposure to the paclitaxel (4 μM) or nocodazole (1 μg/ml) at 37°C, followed by cooling of the cells to 4°C for 10 min, followed by binding of ^{125}I-Tf for 90 min at 4°C.

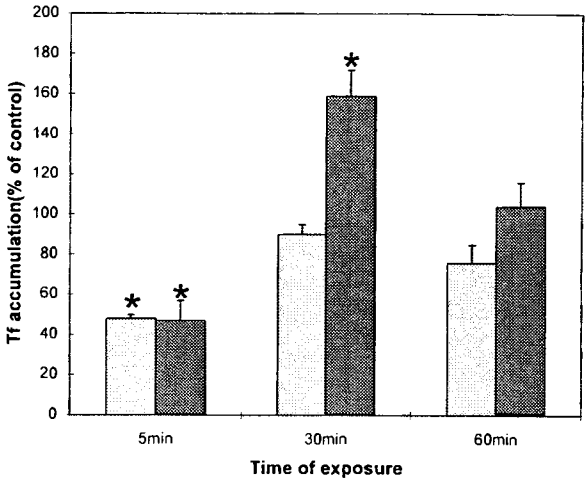

Fig. 3. Differential effects of paclitaxel and nocodazole on ^{125}I-Tf accumulation after different lengths of incubation. Light shaded bars represent paclitaxel treatment and dark shaded bars represent nocodazole treatment. For all treatments, paclitaxel was used at 4 μM and nocodazole was used at 1 μg/ml. All assays involved pretreatment with the drugs at 37°C followed by exposure to ^{125}I-Tf at 37°C for the indicated times (5 min–60 min). Results are expressed as mean ± s.e.m. *Indicates values significant at $p \leq 0.05$. n = 3–5 assays/treatment.

Cellular Localization of Vesicles Labeled with Fluid-phase Fluorescent Markers in Paclitaxel-treated Cells Is Altered

Although neither paclitaxel or nocodazole had altered the amount of uptake of fluid-phase marker, we wanted to determine whether the subcellular localization of fluid-phase markers was altered. Using the fluid-phase fluorescent marker, FITC-BSA, we were able to examine the uptake and distribution of fluid-phase marker at various times in control and paclitaxel- or nocodazole-treated CV-1 cells. The staining patterns of representative cells are shown in Figure 4. Figure 4A shows a typical control cell following 20 min of exposure to FITC-BSA, in which label is distributed relatively uniformly in a punctate vesicular pattern throughout the cell. In contrast, Figure 4B shows a pattern typical of many paclitaxel-treated cells, which was strikingly different from control cells and characterized by redistribution of almost all label to the cell periphery in a punctate pattern with little internal labeling. This pattern was exhibited by 44% of all paclitaxel-treated cells versus only 16% of control cells (Table III). This pattern persisted with increased exposure of the cells to FITC-BSA for up to 90 min (data not shown). In order to see whether this exclusion of fluorescent fluid-phase label to the periphery was specific for paclitaxel-treated cells, we examined the impact of nocodazole-treatment on distribution of internalized marker under the same conditions. Removal of the MT array by nocodazole pretreatment did not result in an overall shift toward peripheral distribution of fluorescent marker relative in controls (Figure 4C and D) Only 6% of nocodazole-treated CV-1 cells exhibited this pre-

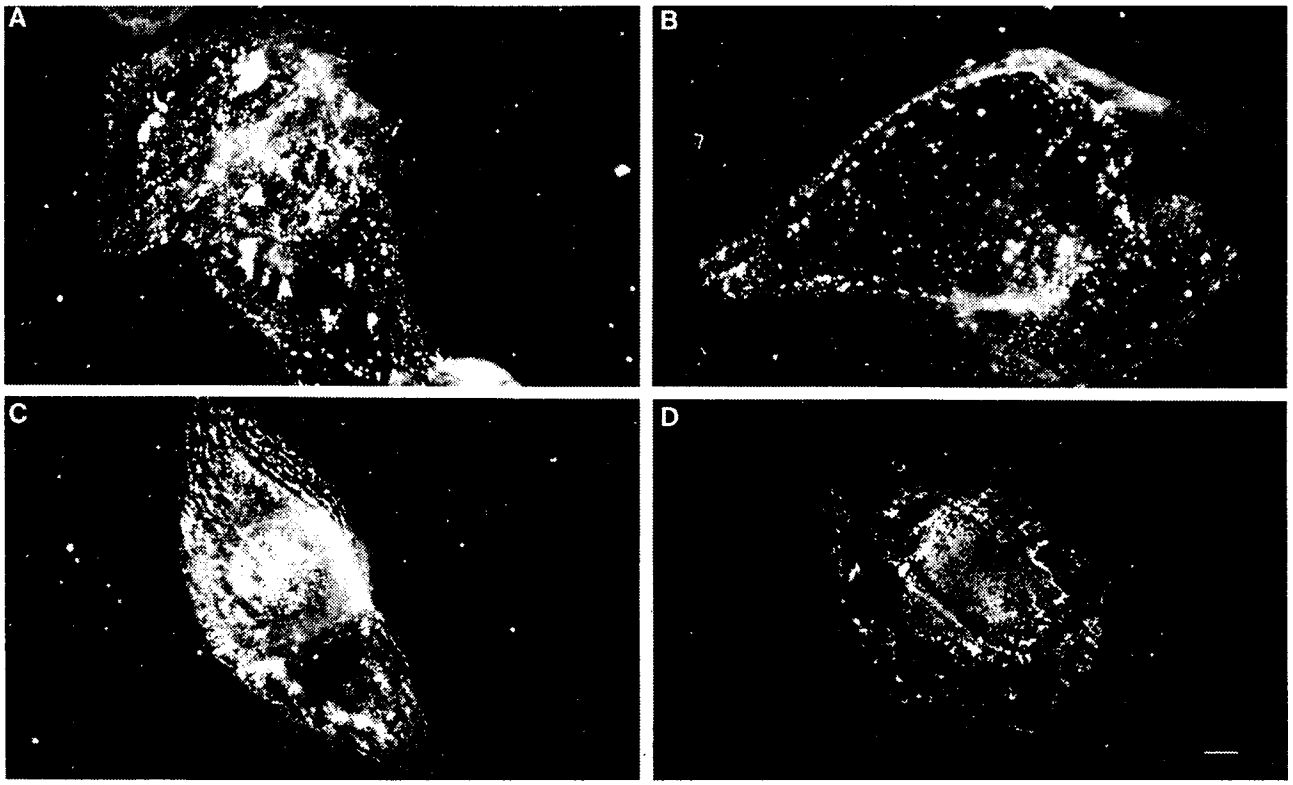

Fig. 4. Paclitaxel but not nocodazole treatment results in a predominantly peripheral distribution of fluorescent fluid-phase marker in CV-1 cells. Subconfluent CV-1 cells were labeled with FITC-BSA in the fluid-phase. A: Paclitaxel control. B: Paclitaxel treated (60 min, 4 μM, 37°C). C: Nocodazole control. D: Nocodazole-treated (60 min, 1 μg/ml, 37°C). All control and treated cells were incubated with FITC-BSA for 20 min, rinsed and fixed as described in Methods. The distribution of fluorescence was analyzed by fluorescence microscopy. Bar is equivalent to 5 μm.

dominantly peripheral labeling pattern (Table 3), in sharp contrast to the paclitaxel-treated morphology.

Lysosomal Distribution Is Significantly Altered by Paclitaxel

In order to further understand how changes in membrane organization might contribute to the effects of paclitaxel and nocodazole on endocytosis, we examined the distribution of the lysosomal network by immunofluorescence microscopy using a monoclonal antibody to LAMP-1. These studies were done in 3T3 cells, since available monoclonal antibody was specific for mouse- or human-derived cells and did not react with our monkey-derived CV-1 cells. We have confirmed that paclitaxel treatment of 3T3 cells elicits comparable reduction in steady state ^{125}I-Tf accumulation: in 3T3 monolayers pretreated for 60 min and then assayed for specific Tf uptake for 90 min, nocodazole-treated (1 μg/ml) 3T3 cells showed accumulation of ^{125}I-Tf that was 113% ± 10% of control while paclitaxel-treated (4 μM) 3T3 cells showed accumulation of ^{125}I-Tf that was 77% ± 8% of control. As shown in Figure 5a, lysosomal membranes in controls are primarily organized in a perinuclear and punctate distribution. The periphery of these cells is almost completely free of punctate staining. In contrast, the distribution of lysosomal membranes in paclitaxel-treated cells (Figure 5a) is altered to a more dispersed staining throughout the cell (Figure 5b). Rather than extending just a short distance from the nucleas, the fluorescence is dispersed almost to the periphery of these cells. The dispersed staining pattern shown in Figure 5b for paclitaxel-treated cells was exhibited in 67% of cells (Table IV). In contrast, this dispersed staining was seen in only 7% of control cells (Table IV). Nocodazole treatment (Figure 5c, Table IV) showed no significant changes in the distribution of lysosomal membranes relative to controls.

Table III. Paclitaxel But Not Nocodazole Reorganizes the Distribution of Fluorescent Fluid-phase Marker to the Cell Periphery

Treatment	Peripheral staining	Perinuclear staining	% of total cells with peripheral staining
Control	39	209	16%
Paclitaxel	66	84	44%
Nocodazole	7	111	6%

Note: Cells were counted randomly from $n = 3$ separate experiments for each treatment. Since no significant differences were observed between paclitaxel controls (receiving DMSO vehicle) and nocodazole controls (exposed to cold for 5 min before receiving DMSO vehicle), these two controls were pooled into one control set.

Paclitaxel-treated Cells Maintained MTs in a Predominantly Radial Array

In order to understand how nocodazole or paclitaxel-induced changes in the MT array might contribute to differences in patterns of accumulation of ^{125}I-Tf, we examined the total

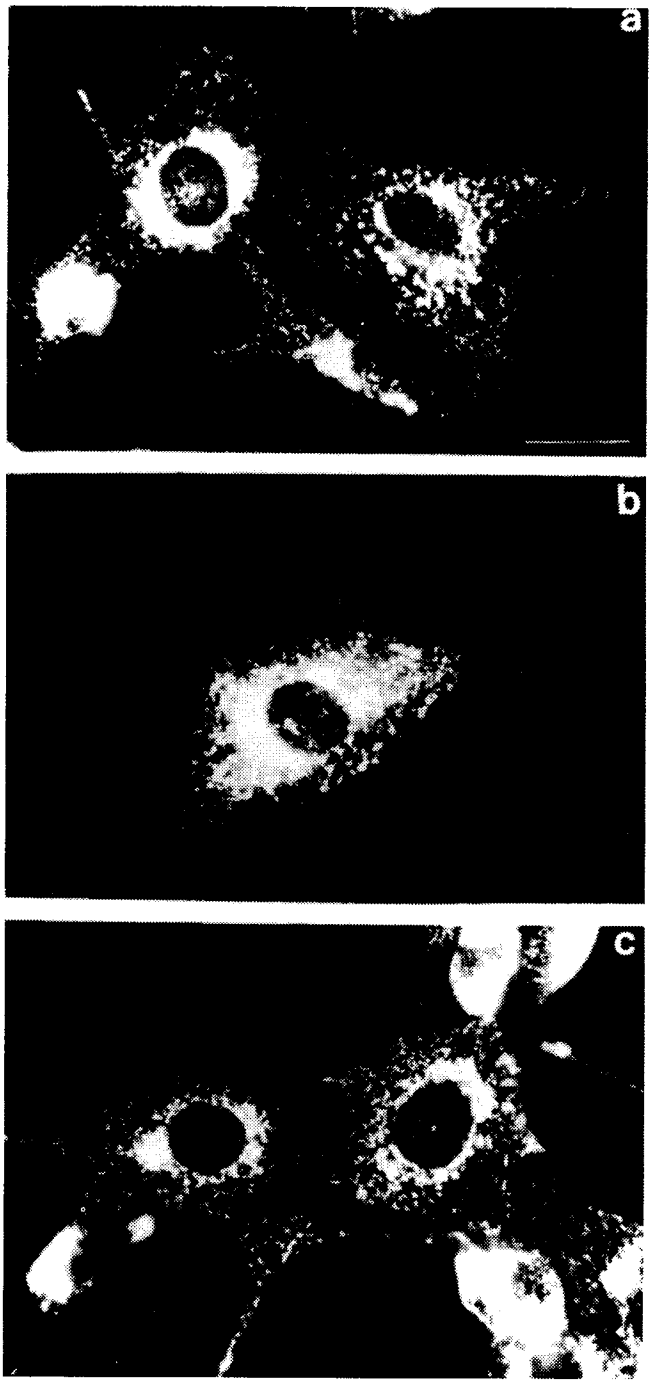

Fig. 5. Paclitaxel but not nocodazole causes a dispersal of lysosomal membranes. Subconfluent 3T3 cells were fixed and processed for immunofluorescence using the monoclonal antibody ID4B to LAMP-1. A: Control. B: Paclitaxel treated (150 min, 4 μM, 37°C). C: Nocodazole-treated (150 min, 1 μg/ml, 37°C). Nocodazole-treated CV-1s were incubated for 5 min on ice prior to addition of drug. Treatment times were chosen to approximate the conditions under which maximal effects on ^{125}I-Tf uptake were seen. Bar is equivalent to 10 μM.

and stable (acetylated) MT array in confluent control, paclitaxel-treated, and nocodazole-treated CV-1 cells by immunofluorescence microscopy. The MT array in control CV-1 cells (Figure 6A) was characterized by a radial distribution of predominantly straight MTs around a single MT-organizing center (MTOC). In contrast, the stable (acetylated) MT array seen in control CV-1 cells (Figure 6B) was characterized by MTs exhibiting a more tangled and less linear morphology, although still organized around a single MTOC. In panels 6C and 6D, it was clear that both the total MT array and the stable (acetylated) MT array were substantially destabilized by nocodazole treatment. However, small fragments of acetylated MTs could still be seen in the CV-1 cells treated with nocodazole after 150 min, indicative of the increased resistance of this particular MT population to nocodazole. Paclitaxel treatment caused accumulation of additional MTs in the total MT array (Figure 6E), although a predominantly radial organization was maintained. The paclitaxel-treated CV-1 cells also exhibited MTs with less of a linear morphology, perhaps reflecting the substantial increases in stable (acetylated) MTs seen in Figure 6F. Of particular interest to the effects of paclitaxel on ^{125}I-Tf uptake, Figures 6E and 6F revealed that paclitaxel-treatment caused MTs to extend parallel to the edge of the cell, rather than perpendicular to it as seen in Figures 6A and 6B. In sum, the nocodazole-treated cells were depleted of essentially all MTs, including stable MTs. The paclitaxel-treated cells showed substantially increased accumulation of MTs, particularly stable MTs, but still maintained MTs in a predominantly radial array around a single MTOC; MTs extending parallel to the edge of the cell could also be seen in the paclitaxel-treated cells but not in controls.

Table IV. Paclitaxel But Not Nocodazole Causes a Dispersal of Lysosomal Membranes

Treatment	Scattered	Perinuclear	% of cells with scattered lysosomes
Control	11	158	7%
Paclitaxel	108	54	67%
Nocodazole	10	135	7%

Note: Cells were counted randomly from $n = 3$ separate experiments for each treatment.

DISCUSSION

An understanding of the basic mechanisms involved in regulation of endocytosis and recycling is a critical first step in designing the appropriate drug delivery strategies for enhancing the uptake and retention of polar drugs. In this study, we have addressed how MT-targeted drugs alter endocytosis, specifically, how changes in the extent of MT assembly generated by paclitaxel and nocodazole impact differently on initial and steady state endocytotic accumulation in cultured cells. These data have shown that neither treatment altered fluid phase endocytosis. However, significant changes in the initial and steady state uptake of ^{125}I-Tf were observed in cells exposed to paclitaxel or nocodazole. Many of the observed changes were different for paclitaxel and nocodazole, suggesting that MT accumulation and MT disassembly have distinct effects on receptor-mediated endocytosis.

The following hypothetical scheme explains our data (Scheme 1). Internalized Tf-TfR has been reported to be distributed throughout early (85%) and late (15%) recycling pathways

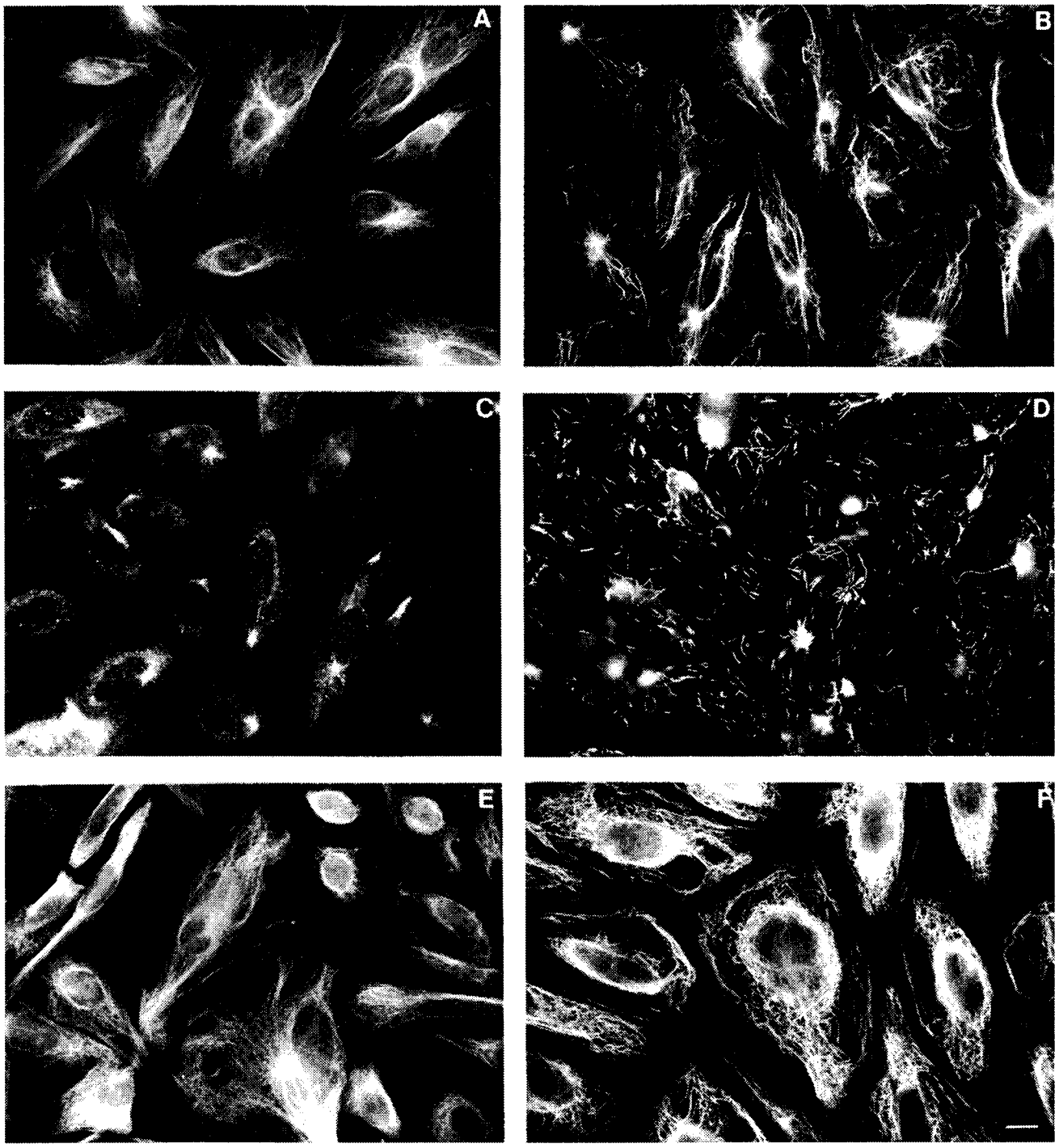

Fig. 6. Under conditions which elicit changes in ^{125}I-Tf accumulation, paclitaxel increases MT content of CV-1 cells, particularly stable MTs while nocodazole treatment causes complete disassembly of the total array and also of stable MTs. Panels A, C, and E were stained with an anti α-tubulin monoclonal antibody (YOL1/34) combined with an FITC-conjugated goat anti-mouse secondary antibody. Panels B, D, and F were stained with an anti acetylated-α-tubulin antibody combined with an FITC-conjugated goat anti-mouse secondary antibody. Panels A and B are control CV-1 cells. Panels C and D are nocodazole-treated CV-1 cells that were cooled for 5 min on ice prior to exposure to 1 μg/ml nocodazole for 150 min at 37°C. Panels E and F are paclitaxel-treated CV-1 cells exposed to 4 μM paclitaxel for 150 min at 37°C. Treatment times were chosen to approximate the conditions under which maximal effects on ^{125}I-Tf uptake were seen. Bar is equivalent to 10 μm.

(12). We can therefore define at least four transport steps involved in the internalization and recycling of Tf-TfR (Scheme 1): Steps 1 and 2 comprise the early pathway while Steps 3 and 4 comprise the late pathway. Step 1 involves the internalization of Tf-TfR from the plasma membrane to the early endosome. Step 2 involves the recycling of the apoTf-TfR from the early endosome to the plasma membrane. Step 3 is defined as the transport of the remainder of the internalized apoTf-TfR to

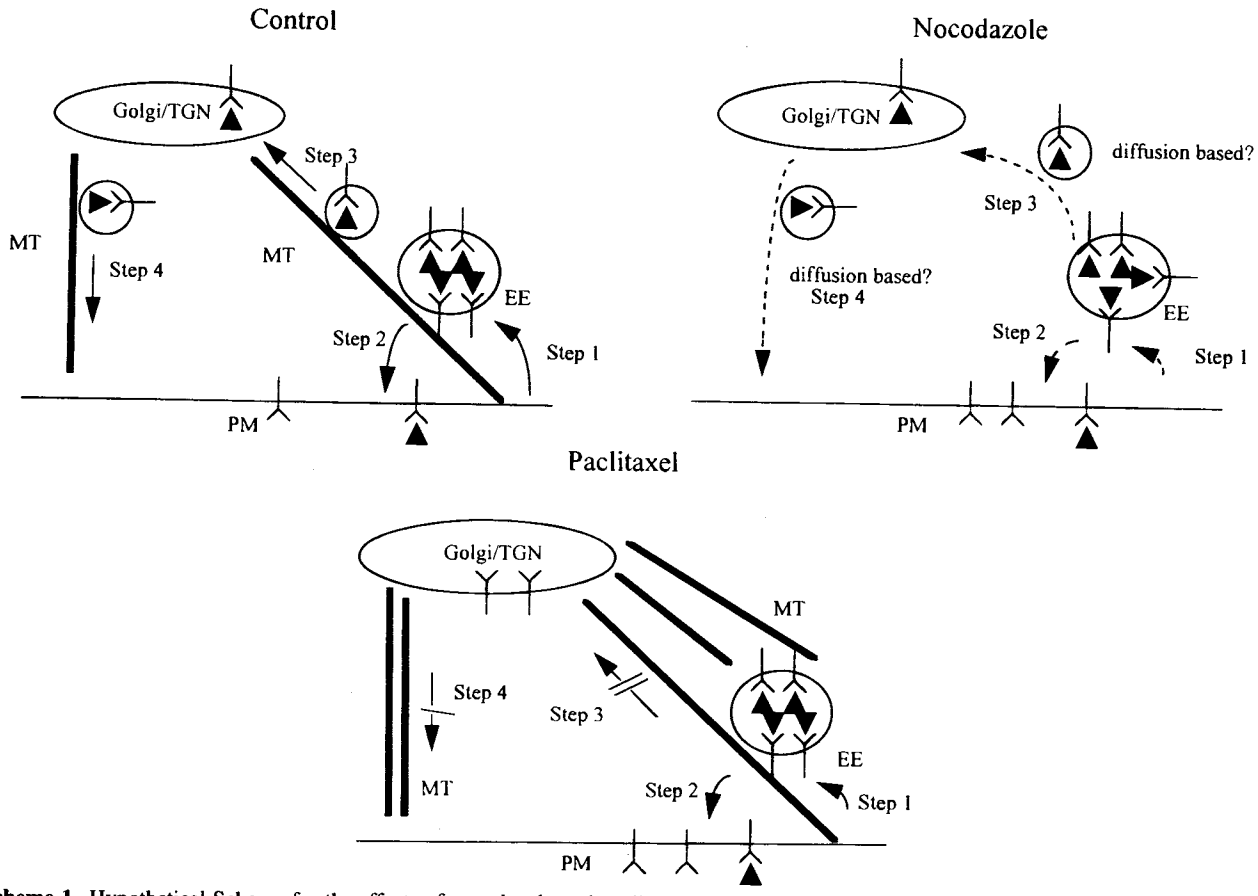

Scheme 1. Hypothetical Scheme for the effects of nocodazole and paclitaxel on Tf accumulation in CV-1 cells. ▼ represents ^{125}I-Tf bound to receptor, so that this receptor is detectable in our binding and uptake assays. EE is early endosome, PM is plasma membrane, MT is microtubule, and Golgi/TGN is the Golgi/trans-Golgi network, the compartment involved in the late pathway of TfR recycling. *Control.* TfR is distributed between the early (EE) and late (Golgi/TGN) pathways. The movement of internalized Tf-TfR between these compartments can be summarized in four steps: Step 1 is the traffic step from PM to EE; Step 2 is the recycling step from EE to PM; Step 3 is the traffic step from EE to Golgi/TGN and Step 4 is the recycling step from Golgi/TGN to PM. *Paclitaxel.* Paclitaxel treatment reduces Step 1 and Step 2. Paclitaxel treatment also uncouples the early recycling (Steps 1 and 2) pathway from the late recycling (Steps 3 and 4) pathway, preventing ^{125}I-Tf bound to TfR from entering the late recycling pathway. Since the early recycling pathway is much shorter than the late pathway, the increase in radioactivity due to ^{125}I-Tf passage through the late recycling pathway is missing in paclitaxel-treated cells relative to controls. Paclitaxel pretreatment causes a reduction in the surface receptor available for binding ^{125}I-Tf by inhibition of Step 4 during pretreatment. We suggest that these receptors are trapped in the late pathway during pretreatment, and are "silent" in our assays because they have no access to ^{125}I-Tf. *Nocodazole.* Nocodazole treatment reduces Step 1 and Step 2. However, traffic can proceed through Steps 1–4 at a reduced rate in the absence of MTs, possibly through a diffusion-based process.

the Golgi complex. Step 4 is defined as the recycling of the apoTf-TfR complex from the Golgi to the plasma membrane. We have previously shown that movement of components from the Golgi apparatus to the plasma membrane is inhibited by paclitaxel (24), suggesting that Step 4 is MT-dependent. Other studies have suggested that Step 3 is also MT-dependent (1) and sensitive to paclitaxel treatment (25).

Monensin has been reported to impact on receptor internalization and recycling (reviewed in 22); specifically, monensin inhibits TfR recycling through the Golgi (23) and causes accumulation of internalized ^{125}I-Tf(26). A MT-independent block in traffic from the Golgi is consistent with the intracellular accumulation of ^{125}I-Tf that we observe after 90 min of uptake in the presence of monensin, similar to a previous report (26). These data suggest that a block in traffic from the Golgi (Step 4) by either paclitaxel or nocodazole should promote accumulation of ^{125}I-Tf at 90 min, which is not observed with either treatment.

Our interpretation of the effects of nocodazole is shown in Scheme 1 (*Nocodazole*). We found that nocodazole reduced the initial uptake of ^{125}I-Tf at 5 min, suggesting an effect on Step 1. Once internalized, the Tf-TfR complex can be recycled (Step 2) or continue through the later pathway (Step 3). The slight increase in plasma membrane TfR that we observe following nocodazole pretreatment is also consistent with our findings that receptor uptake through Step 1 is inhibited, as well as the findings of a previous study which also reports increased TfR content of the plasma membrane following nocodazole pretreatment (12). The mechanism underlying the decreased uptake of plasma membrane TfR by nocodazole is unknown, but may involve a requirement for MTs in organization of membrane domains or coated pits.

The observation that nocodazole treatment causes a significant increase in ^{125}I-Tf accumulation after 30 min despite the reduced uptake at Step 1 suggested that recycling or sorting at Step 2 is also reduced. Since nocodazole-treated cells regained control levels of ^{125}I-Tf accumulation after 90 min, it is likely that the bolus of internalized ^{125}I-Tf at 30 min is gradually processed by diffusion-based transport through Steps 3 and 4 or alternatively, gradually through Step 2. It is more likely that Tf-TfR traffic from the early endosome proceeds through Steps 3 and 4 by diffusion-based transport, based on previous work (12) showing that nocodazole causes no effect on the traffic to the Golgi apparatus.

Scheme 1 (*Paclitaxel*) summarizes our hypothesis for the effects of paclitaxel on TfR trafficking in CV-1 cells. We have observed that paclitaxel also reduced the initial uptake of ^{125}I-Tf at 5 min, suggesting an effect on Step 1 similar to that of nocodazole. These results with paclitaxel, like those with nocodazole, reinforce that a MT-sensitive step is involved in initial events in receptor-mediated endocytosis. Little reduction in net ^{125}I-Tf accumulation was found after 30 min, suggesting that the initial deficit in uptake at 5 min may be accompanied by a reduced rate of recycling in Step 2.

There is no net accumulation of ^{125}I-Tf in paclitaxel-treated cells at 30 minutes as in nocodazole-treated cells nor is there net accumulation of ^{125}I-Tf at 90 min as in monensin-treated cells. This difference suggests that the ^{125}I-Tf in the early endosome is not further internalized, since processing via Step 3 should result in accumulation of ^{125}I-Tf in the Golgi apparatus and a concomitant increase in ^{125}I-Tf relative to control, consistent with previous studies showing a block in Golgi-derived traffic by paclitaxel (24). Failure of receptor-containing vesicles to move inward from the early endosome on paclitaxel-stabilized MTs is supported by a previous study (25). We hypothesize that paclitaxel uncouples the early (Step 1 and Step 2) and late (Step 3 and Step 4) recycling pathways for TfR such that ^{125}I-Tf in paclitaxel-treated cells has no access to perinuclear compartments via Step 3 and Step 4. The reduction in accumulation that occurs at steady state from 30–90 min in paclitaxel-treated cells relative to control cells is due to the gradual partitioning of ^{125}I-Tf throughout the late pathway in control cells, which does not occur in paclitaxel-treated cells. The ^{125}I-Tf retained in the late endosomal pathway in controls is instead recycled through Step 2, causing the difference in the relative retention of ^{125}I-Tf in control versus paclitaxel-treated cells to increase with time.

The reduction of Tf accumulation over time is almost certainly enhanced by a gradual sequestration of TfR present in cellular compartments during pretreatment with paclitaxel; this hypothesis is supported by the reduced plasma membrane TfR caused by paclitaxel (Table II). Loss of approximately 15% of TfR at the plasma membrane through sequestration in the Golgi by paclitaxel is consistent with the known parameters for TfR exchange from the plasma membrane (28). Since paclitaxel reduces traffic from the Golgi apparatus, TfR present in the late pathway during pretreatment would be expected to be sequestered due to inhibition of Step 4 by paclitaxel. Our finding on the predominantly peripheral localization of internalized fluorescent fluid-phase marker in paclitaxel-treated cells is also consistent with the hypothesis that paclitaxel prevents the inward movement of early endosomal components from the periphery to the cell interior.

A major question generated from this study is why paclitaxel-induced MT stabilization alters the ability of MTs to sustain vesicle transport and sorting from the early endosomes. One major change is the shift in the MT array toward increased numbers of stable MTs in the presence of paclitaxel (Figure 6). Little is known about the function of stable MTs, except that they are associated with organelles such as the Golgi apparatus (29) that maintain a distinct location within cells. Perhaps their function is to provide a scaffold for anchorage but not movement of membranes. In contrast, dynamic MTs are normally distributed in a radial array extending into the peripheral regions of the cell where most of the MT-dependent vesicle transport occurs. Perhaps dynamic MTs normally mediate endosomal sorting and processing from early to late recycling pathways. Paclitaxel-induced increases in peripheral stable MTs may lead to the inhibition of the movements of membrane vesicles involved in endocytosis that are normally transported along dynamic MTs. Although no quantitative effects were observed on fluid-phase uptake, a morphological effect consistent with peripheral sequestration of endosomal constitutents is illustrated in the paclitaxel-treated cells in Figure 4.

Uptake of a polar drug is not necessarily sufficient to enhance cellular retention. The time spent in the endocytotic pathway in many cases governs the ability of a drug to traverse the endosomal membrane barrier and reach the cytoplasm. In some cases, transient delays in endosomal processing which increase the residence time of drug in the endosomal pathway can enhance cellular accumulation of drug (30). Our study shows that modulation of the extent of MT assembly and of the distribution of MT subpopulations can have remarkable effects on receptor-mediated endocytosis. In the case of MT disassembly, intracellular accumulation of Tf relative to controls was enhanced at earlier time points but returned to steady state after 60–90 min. Such a situation would be advantageous in prolonging the residence time of a polar drug complexed to ligand in the endosomal pathway. In contrast, MT assembly caused decreased accumulation of Tf relative to controls. This finding suggests that administration of paclitaxel to cells following exposure to drug complexed to ligand might likewise increase the intracellular residence time. This may constitute a general strategy for enhancing the efficacy of chemotherapeutics, through administration of MT-targeted chemotherapeutic drugs like paclitaxel and colchicine in combination with other therapeutics which could be targeted by receptor-mediated endocytosis. However, other drug or non-drug based regulatory strategies for locally manipulating MT content may be useful in transiently altering endocytotic uptake and recycling to enhance drug delivery, similar to the use of monensin for enhancement of the efficacy of immunotoxins in cancer therapy (30).

ACKNOWLEDGMENTS

Dr. Austin Mircheff, Dr. Curtis Okamoto, and Dr. Maria Runnegar are thanked for many helpful discussions. Xinhua Wei is also thanked for excellent technical assistance. The authors thank Dr. Janet Blanks at the Doheny Eye Institute, USC for providing access to facilities. This study was supported by NIH grant CA 63387 and a New Investigator Award from the AACP/Burroughs Wellcome Fund to SHA. SHA is an Initial Investigator of the American Heart Association-Greater Los Angeles Affiliate.

REFERENCES

1. S. F. Hamm-Alvarez. *Pharm. Res.* **13**:489–496 (1996).
2. N. B. Cole and J. Lippincott-Schwartz. *Curr. Op. Cell Biol.* **7**:55–64 (1995).
3. P. B. Schiff, J. Tant, and S. B. Horwitz. *Nature (Lond.)* **22**:665–667 (1979).
4. S. F. Hamm-Alvarez, P. Y. Kim, and M. P. Sheetz. *J. Cell Sci.* **106**:955–966 (1993).
5. M. de Brabander, B. Guens, R. Nuydens, R. Willebrords, F. Aerts, and J. de May. *Int. Rev. Cytol.* **101**:215–274 (1986).
6. H. A. Huebers and C. A. Finch. *Physiol. Rev.* **67**:520–582 (1987).
7. M. D. Snider and O. C. Rogers. *J. Cell Biol.* **100**:826–834 (1985).
8. M. D. Snider and O. C. Rogers. *J. Cell Biol.* **103**:265–275 (1986).
9. J. W. Woods, M. Doriaux, and M. G. Farquahar. *J. Cell Biol.* **103**:277–286 (1986).
10. M. de Brabander, R. Nuydens, H. Geerts, and C. R. Hopkins. *Cell Motil Cytoskel* **9**:30–47 (1988).
11. P. Pierre, J. Scheel, J. E. Rickard, and T. E. Kreis. *Cell* **70**:887–900 (1992).
12. M. Jin and M. D. Snider. *J. Biol. Chem.* **268**:18390–18397 (1993).
13. W-C. Shen, J. Wan, and H. Ekrami. *Adv. Drug Deliv. Rev.* **8**:93–113, (1992).
14. E. Wagner, D. Curiel, and M. Cotton. *Adv. Drug Deliv. Res.* **14**:113–135 (1994).
15. V. I. Gelfand and A. D. Bershadsky. *Annu. Rev. Cell Biol.* **7**:93–116 (1991).
16. A. J. Winder, A. Wittbjer, E. Rosengren, and H. Rorsman. *J. Cell Sci.* **106**:153–166 (1993).
17. *Worthington Enzyme Manual*, Worthington Biochem. Co., Freehold, N. J., pp. 43–45 (1972).
18. J. Larrick and P. Cresswell. *Biochim. Biophys. Acta.* **583**:483–490 (1979).
19. J. Wan, M. E. Taub, D. Shah, and W-C. Shen. *J. Biol. Chem.* **267**:13446–13450 (1992).
20. D. K. Wilcox, R. P. Kitson, and C. C. Widnell. *J. Cell Biol.* **92**:859–64 (1982).
21. S. C. Silverstein, R. M. Steinman, and Z. A. Cohn. *Annu. Rev. Biochem.* **46**:669–722 (1977).
22. J. J. Mollenhauer, D. J. Morre, and L. D. Rowe. *Biochim. Biophys. Acta.* **1031**:225–246 (1990).
23. Stein, K. G. Bensch, and H. H. Sussman. *J. Biol. Chem.* **259**:14762–14772 (1984).
24. S. F. Hamm-Alvarez, B. Alayof, H. Himmel, P. Y. Kim, A. L. Crews, H. C. Strauss, and M. P. Sheetz. *Proc. Natl. Acad. Sci. USA* **91**:7812–7816 (1994).
25. P. M. Novikoff, M. Cammer, L. Tao, H. Oda, R. J. Stockert, A. W. Wolkoff, and P. Satir. *J. Cell Science* **109**:21–32 (1996).
26. J. H. Mehringer and S. E. Cullen. *J. Immunol.* **145**:2064–2069 (1990).
27. H. S. Thatte, K. R. Bridges, and D. E. Golan. *J. Cell Physiol.* **160**:345–357 (1994).
28. C. Watts. *J. Cell Biol.* **100**:633–637 (1985).
29. J. Thyberg and S. Moskalewski. *Cell Tissue Res.* **273**:457–466 (1993).
30. T. Griffin, M. Rybak, L. Recht, M. Singh, A. Salimi, and V. Raso. *J. Natl. Cancer Inst.* **85**:292–298 (1993).